



## HIGH-LIFT SURFACES DEFLEXION FOR LOW-SPEED AIRFOIL

**Roberto M. Girardi**

**Pedro Paglione**

Instituto tecnológico de Aeronáutica (ITA)

Praça Mal. Eduardo Gomes, 50

12.228-900 São José dos Campos, SP, Brasil

**Abstract.** *The relative angles and the leading edge positions of a slat and a flap are obtained in order to maximize the lift coefficient of a multi-element airfoil. The flow over this complex configuration is calculated through a viscous-non-viscous interaction procedure. The potential flow is determined by using a panel method based on the tangent dipole and on the vortex singularities associated with the stream function, which is used to impose the boundary condition. The boundary layer on the surface of each element is calculated through a computational code based on the integral equations. Such code is capable of analyzing laminar and turbulent flows and furnishing the friction coefficient and the displacement thickness, which is used to perform the viscous-non-viscous coupling. Two cases are analyzed and compared: a three-element airfoil and a flap-airfoil configuration.*

**Key words:** *Potential flow, Boundary layer, Optimization technique, Three-element airfoil.*

### 1. INTRODUCTION

During some airplane operations, higher values of the lift coefficient ( $C_l$ ) are interesting in order to fly at lower velocities. This is the case of take off and landing situations, where high-lift devices are used, such as flaps and slats (leading edge flaps). These devices are normally commanded by the airplane pilot, but in some cases an automatic operation is desirable, as for agricultural airplanes, because their operations require several curves of  $180^\circ$ , in order to spread agricultural products on an area of interest. Such curves must be as small as possible and have to be achieved at small velocities and with high lift coefficient.

The motivation of the present work is to obtain information for designing a simple high-lift device, which could be used in agricultural airplanes. This information can be obtained by using aerodynamic optimization and is very important to calculate the forces and moments acting on the slat and on the flap surfaces, which will be used to specify the mechanical device characteristics. The aerodynamic optimization mentioned above is performed numerically and the panel method is used to calculate the potential flow over a complex configuration. From the numerical point of view, the main concern when multielements have to be calculated is the

problem arising when one element is very near the other, as is the case for the configuration of the present work. The classical Hess & Smith (1966) scheme, with constant strength source and vortex panels, presents the above problem. In this work, a new scheme based on the tangent dipole singularity is used for the case of multi-element configuration. This method was already applied to a two-element configuration (profile with a flap) and good results were obtained, as can be seen in Girardi & Silva (1994).

The boundary layer flow is obtained by using the integral equation method, developed by Rotta (1971). The viscous-non-viscous coupling is made through a transpiration procedure, where new values for the normal velocity (different from zero) are used to enforce the boundary conditions, on the profile surface, in the potential flow calculation. These new values are obtained from the displacement thickness distribution, determined by the boundary layer code.

## 2. NUMERICAL METHOD

The numerical method used in this work can be divided in two basic parts: (i) The first one is the calculation of the flow over a multi-element airfoil, where the potential flow is coupled to the boundary layer solution by using the transpiration procedure and (ii) the second part is the use of an optimization technique, which calls the first part in order to find the maximum lift coefficient for the configuration.

### 2.1 Panel Method

In the potential flow over a profile, the Laplace equation must be solved subjected to boundary conditions at infinity (which are automatically satisfied by the singularity method) and on the profile surface. In the so-called direct problem, the boundary condition on the profile surface can be imposed in two different ways: The normal velocity must be zero or the stream function ( $\Psi$ ) has a constant value on the profile surface.

For the numerical method developed in this paper, the tangent dipole panel was chosen for the flow modeling and the stream function is used to enforce the boundary condition. This choice guarantees a dominant main diagonal for the influence coefficient matrix and a well conditioned numerical problem. Two difficulties arise immediately due to the stream function use as boundary condition: (1) it can be shown (see Hunt, 1978) that for the external flow problem the tangent dipole distribution is not unique. Hence, the influence coefficient matrix is singular. (2) The stream function value, which must be imposed on the profile surface as the boundary condition, is a function of the circulation as can be seen in Lamb (1932). Therefore, this stream function value is an unknown of the problem because the circulation value is unknown "a priori". The first difficulty can be overcome by fixing one value for the tangent dipole distribution, as discussed by Hunt (1978). Specifically for the panel method developed in this work, the last panel (number N) density is initially fixed with a unit value ( $\mu_N=1$ ). Considering the above reasoning, the stream function at an arbitrary control point ( $Z_{c_k}$ ) is given by

$$\Psi_k = \sum_{j=1}^{N-1} \text{Im}[F_{kj}^d] \mu_j + \text{Im}[F_{kN}^d] \cdot 1 + \gamma \sum_{j=1}^N \text{Im}[F_{kj}^v] + \text{Im}[V_\infty e^{-i\alpha} (Z_{c_k} - Z_R)]$$

for  $k=1,2,\dots,N$  (1)

where  $V_\infty$  is the free stream velocity,  $\alpha$  is the angle of attack and  $F_{kj}$  is the complex potential induced at the control point of a panel  $k$  ( $Z_{ck}$ ) due to a panel  $j$ , which has a unit distribution density ( $\mu_j=1$ ). The superscripts "d" and "v" indicate, respectively, that the complex potential is due to tangent dipole and vortex panels. The parameters  $F_{kj}$  can be found in Girardi (1999) and  $Z_R$  is a reference point, where the complex potential is made equal to zero, as discussed by Girardi (1999).

A constant value for the stream function ( $\bar{\Psi}$ ) must be imposed at the control points of all the panels, in order to satisfy the boundary condition on the profile surface. Hence, equation (1) is a system of  $N$  equations, relating  $N-1$  tangent dipole densities ( $\mu_j$ ;  $j=1, 2, \dots, N-1$ ) and one vortex density ( $\gamma$ ). On the other hand, the Kutta condition must be considered and the above unknowns are related by one more equation. Therefore,  $N+1$  equations must be used to obtain  $N$  unknowns.

Considering the above problem, the second difficulty can be naturally solved. As the stream function value ( $\bar{\Psi}$ ) is unknown "a priori", it can be considered as the unknown that is lacking for the above problem to become a determinate one, that is,  $N+1$  equations and  $N+1$  unknowns.

In the present work, the Kutta condition is imposed in the way used initially by Hess & Smith (1966), where the tangent velocity at the panels adjacent to the trailing edge are considered equal.

A problem that is normally found in the flow calculation over a profile is the treatment of the trailing edge shape, which can be sharp or blunt (which is the normal case, due to practical reasons). In the case of a blunt trailing edge, the discretization has to be open (the surface of the trailing edge base is not considered) or it has to be artificially closed by using additional panels (Bristow & Goose, 1978). In the numerical method developed in the present work the problems associated to an open discretization can be minimized. As mentioned before, due to the non-uniqueness of a tangent dipole distribution for external flows, one of the panel strengths has to be specified and in the present method the panel number  $N$  was chosen. As mentioned above, its value was specified initially equal to unit. Meanwhile, this value is arbitrary and for an open discretization a value lesser than  $10^{-4}$  is required in order to avoid numerical problems, associated with abrupt panel strength variations at the trailing edge of a profile, as shown by Girardi (1994).

For the case where the lift force (circulation) is different from zero and an open discretization is implemented, it is necessary to analyze the vortex distribution to avoid numerical problems at the trailing edge. The classical way to introduce circulation around a profile is through a constant vortex distribution. However, to treat the case of an open discretization it is necessary to prescribe other distribution, where the vortex strength tends smoothly to zero for the panels at the trailing edge (panel numbers 1 and  $N$ ). As in Girardi & Bizarro (1998), a cubic distribution was chosen for defining a weight function (WF) and, then, the vortex distribution is given by

$$\gamma_j = WF_j \cdot \bar{\gamma} \quad (2)$$

where  $\gamma_j$  and  $WF_j$  are, respectively, the circulation density and the weight function value of each panel along the profile surface and  $\bar{\gamma}$  is a constant and, in fact, it is the only unknown of the circulation distribution. With this new distribution, the stream function at a panel  $k$  (given by eq. 1) has to be rewritten in the following form

$$\Psi_k = \sum_{j=1}^{N-1} \text{Im}[F_{kj}^d] \mu_j + \text{Im}[F_{kN}^d] \mu_N + \bar{\gamma} \sum_{j=1}^N \text{Im}[F_{kj}^v] \cdot \text{WF}_j + \text{Im}[V_\infty e^{-i\alpha} (Zc_k - Z_R)]$$

for  $k=1, 2, \dots, N$  (3)

## 2.2 Boundary Layer and Potential Flow Coupling

In this work, the boundary layer flow is obtained through the numerical method implemented by Rotta (1971). In such a method, the boundary layer equations in the integral form are used for calculating laminar and turbulent flows. Michael criteria (see Schetz., 1984) was implemented for determining the laminar-turbulent transition and good results were obtained.

As is well known, the pressure coefficient obtained from the potential flow solution (panel method) has to be used for the boundary layer calculation. Meanwhile, the results obtained with the potential flow code have to be adapted, in order to be read by the boundary layer code. Initially, the stagnation point location has to be determined on the profile surface, because the boundary layer calculation is started at this point. Then, the boundary layer code is called two times, once for calculating the upper surface and the other for the lower surface.

Two boundary layer code results are used in the present work: (i) the friction coefficient, for determining the friction drag through an integration along the profile surface and (ii) the displacement thickness, which is used to perform the coupling with the potential flow. Such coupling can be accomplished by implementing new values for the normal velocity (potential flow boundary condition), which models the boundary layer growth, through a transpiration effect. In the transpiration procedure, the normal velocity at the control point of each panel is a function of the displacement thickness growth, as shown in Bizarro (1998). In the same reference, a problem occurring at the trailing edge region is discussed, which is caused by an explosive growth of the displacement thickness. This problem can be minimized by a procedure presented in Bizarro (1998).

After the new boundary condition enforcement, the potential flow code gives a new pressure coefficient distribution, which is used to calculate the lift coefficient and the pressure drag. The total drag coefficient is then obtained considering the friction and the pressure items.

When flow separation is detected by the boundary layer code, such information is transferred to the main program, in order to be used by the optimization code.

## 2.3 Optimization Method

The optimization techniques can be mathematically stated as the following optimization problem:

$$J = \max[F(x)]$$

$$\text{subject to } g_i(x), \quad i = 1, 2, \dots, q \quad (4)$$

where  $x$  is a vector containing the design variables and  $J$ , figure of merit of this problem, is the maximum lift coefficient for the three element configuration. The term  $g_i(x)$  defines all the p-constraints pertinent to the problem as described below.

For obtaining the optimal profile configuration according to a specific aerodynamic figure of merit (maximal lift coefficient, maximal boundary layer transition, minimal drag coefficient, etc) which serves as the objective function, the numerical optimization procedure

Globex is used in this work, implemented by Jacob (1982). It employs a robust local minimization algorithm of a real valued function of several variables that converge quickly to the nearest relative extreme point and is insensitive to curved valleys and sharp ridges in the variables-criterion space. It can handle any type of constraint with no need for gradient evaluation since each time a constraint violation is detected, the optimization algorithm is signaled to provide a new set of variables until a set is obtained that violates no boundary.

For aerodynamic optimization this is an advantageous strategy, besides its simplicity, since the gradients evaluation could have a prohibitive computational cost due to iterative procedures or even impossible in some particular cases. The global extreme of the function is reached, with great likelihood, through the use of a three step procedure based on a normally distributed random number. In the first step, the initial values of the variables are estimated. The vectorial mean value of these normally distributed points as well the mean quadratic deviation is derived from the user initial points given. In each one of these points, a local extremization procedure is started. In the second step, around the variables that resulted in the best function value, once more normally distributed random numbers are generated and in each one of the these points a new local optimization is calculated. Once a better function value is found, this point is used as the new mean value for another random search and the mean quadratic deviations are multiplied by 0.9 (localization of the global extreme). The best value of all in these steps is stored and used as the initial value for a third optimization step. Although the global extreme can not be determined with absolute security, the probability is found to increase with the number of random estimated values.

### 3. RESULTS

The methodology adopted in this paper was applied to a two and three element configuration. The two element airfoil, constituted by the main element and its flap, was originated from a MS 0313 airfoil. The three-element configuration was derived from the same airfoil and the slat shape developed by Girardi & Silva (1994).

The results presented below were obtained after the optimization procedure was applied for each angle of attack of the configuration, which is defined as the angle between the undisturbed flow and the main element chord line.

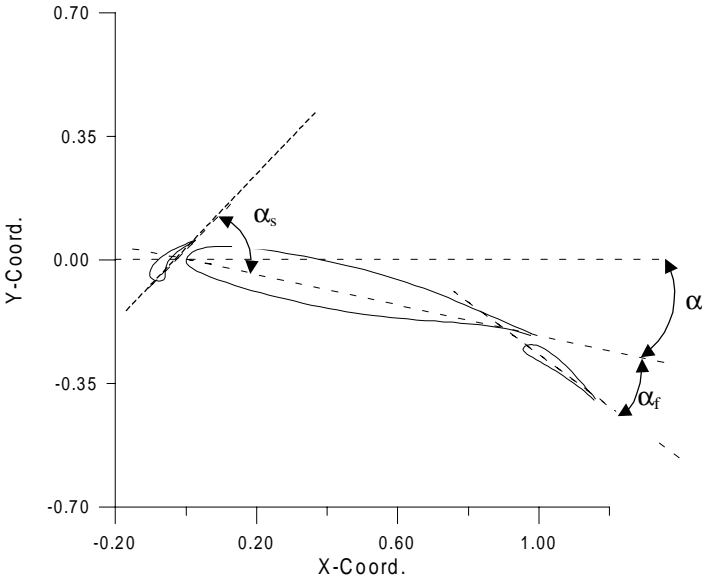


Figure -1 Three-element configuration.

A decrease of the Flap angle of attack ( $\alpha_f$ ) for the two element airfoil, while the configuration angle of attack ( $\alpha$ ) is incremented, can be observed in the Fig. 2. For lower values of  $\alpha$  the only way for maximize the configuration lift coefficient is to increment  $\alpha_f$ . On the other hand, the increment of  $\alpha_f$  is limited by the boundary layer separation on the upper surface of the flap, which can be detected by the boundary layer code utilized in this work and, as mentioned before, this is one of the constraints imposed by the optimization technique. The high values obtained for  $\alpha_f$  indicate that the interference between the main element and the flap is very effective for preventing flow separation for lower  $\alpha$  values. As is well known, this effect is caused because airflow coming from the main element lower surface is directed to the flap's upper surface by the gap between the airfoil elements. The interference effect decreases while  $\alpha$  is incremented, because a decrease of  $\alpha_f$  is observed and this is caused by the flow separation on the flap surface.

During the optimization procedure, the flap leading edge position is varied to obtain the maximum Cl value for each angle of attack of the main element. This position is defined by the X and Y coordinates, relative to a reference system whose origin is located at the main element leading edge and which rotates with the configuration, in such a way that the X-axis is always coincident to the main element chord line.

In the Fig. 3, it is possible to observe that in the range for  $\alpha$  between 0 and approximately 10 degrees there is an increment of the X-coordinate and a maximum is reached for  $\alpha$  equal to 10 degrees. In the same range the Y-coordinate is approximately constant. These results indicate that the flap leading edge is moved backward in a direction parallel to the main element chord line. For angles of attack ( $\alpha$ ) greater than 10 degrees, the flap leading edge has to be moved downward and forward, as can be seen in the Figs. 4 and 3, respectively.

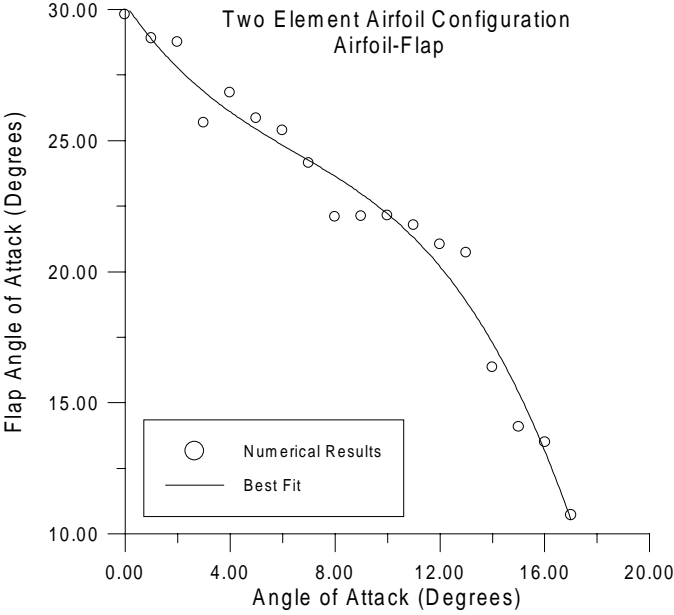


Figure –2 Flap angle of attack for a two-element airfoil.

For the three-element configuration, the flap ( $\alpha_f$ ) and slat ( $\alpha_s$ ) angles of attack (see Fig. – 1) are shown in the Fig. - 5 as a function of  $\alpha$ . As for the case of a two-element configuration, the flap angle of attack decreases while  $\alpha$  is increased, but the decrement of  $\alpha_f$  is less pronounced for the three-element configuration. The slat angle of attack is almost constant, with a value near –17 degrees.

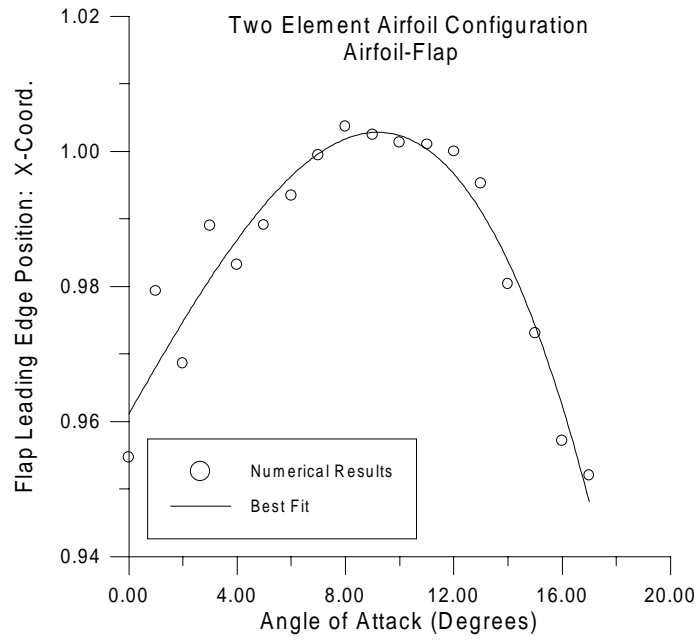


Figure –3 Flap leading edge position (X coordinate) for a two element airfoil

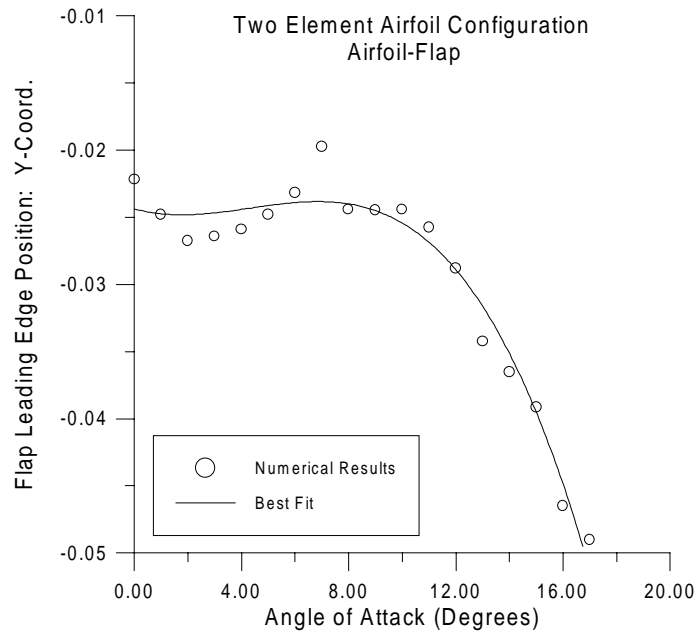


Figure –4 Flap leading edge position (Y coordinate) for a two element airfoil

The leading edge positions for the flap and for the slat are shown in the Figs. 6 and 7, where X and Y coordinates are presented as a function of the configuration angle of attack. On the contrary to the two element airfoil (see Fig. 3), the X coordinate of the flap leading edge does not have a maximum value and, in fact, is approximately constant. Comparing Figs. 7 and 4, one can see that the Y coordinate of the flap leading edge varies in a similar manner for the two and three element configurations. Therefore, for the three-element configuration the flap has to be moved only downward and this is an interesting result because the flap movement mechanism can be simplified. As can be seen in the Figs. 6 and 7, the slat leading edge position is almost constant up to the angle of attack considered, which is limited to situations where the boundary-layer separation is not allowed. The X coordinate for the slat leading edge position

is near  $-0.25$  (see Fig. 6), which was the forward limit for this coordinate. This result indicates that the extreme condition (maximum  $Cl$ ) is reached when the slat is moved far from the main element. This occurs because the slat causes a decrement on the pressure coefficient peak on the main airfoil upper surface, near its leading edge, which is responsible for a decrement of the configuration  $Cl$ . On the other hand, the same influence on the pressure distribution is responsible for preventing boundary-layer separation on the upper surface of the main element and delaying the three-element airfoil stall.

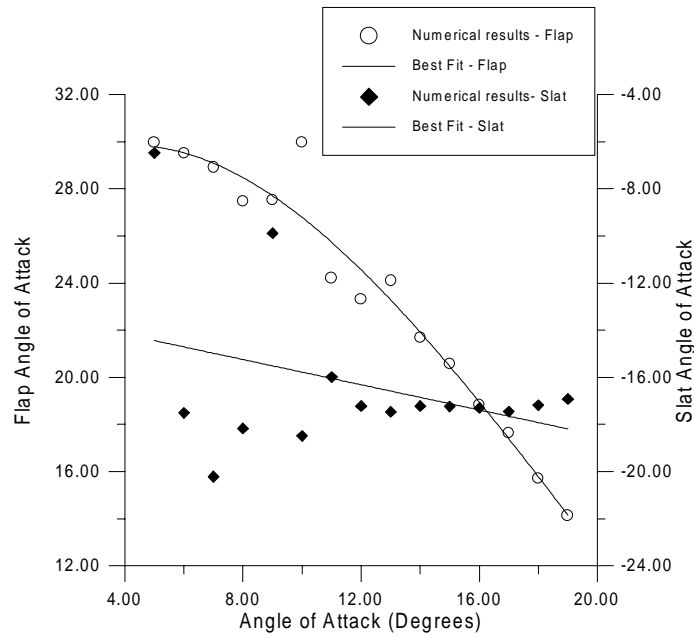


Figure – 5 Angle of attack for the flap and for the slat of a three element airfoil

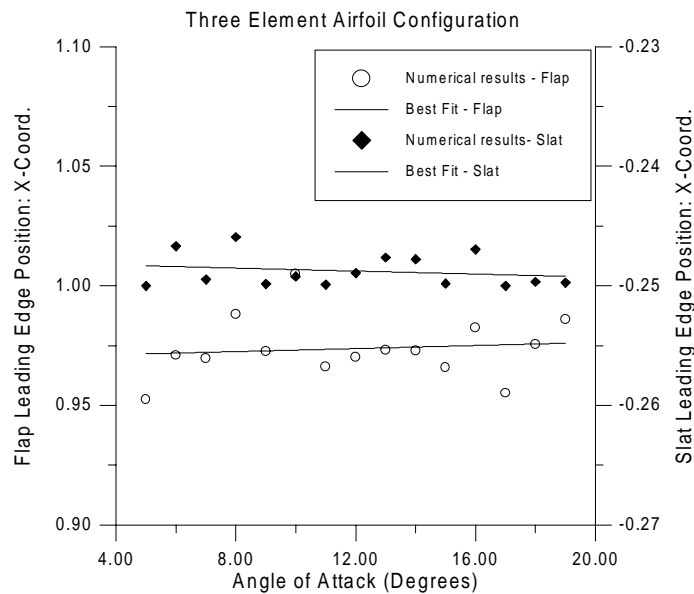


Figure –6 Leading edge position (X coord.) for the flap and for the slat of a three element airfoil

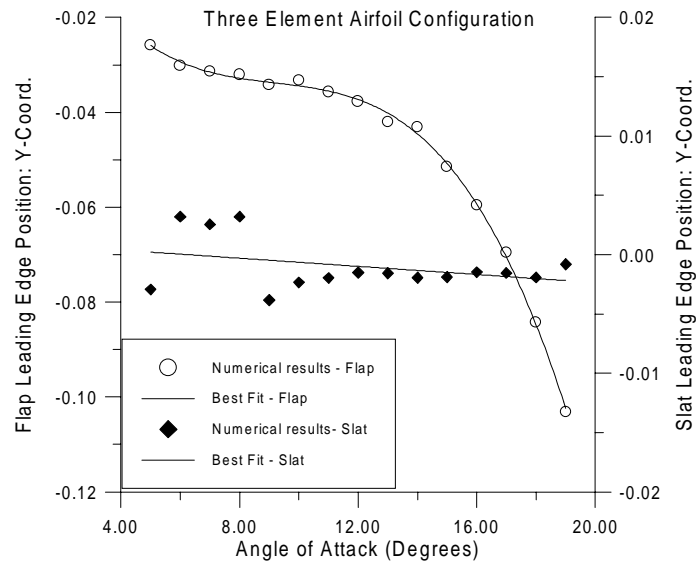


Figure –7 Leading edge position (Y coord.) for the flap and for the slat of a three element airfoil

The maximum lift coefficient ( $C_{l_{max}}$ ) for each angle of attack is presented in Fig. 8, where the two and three element configurations are compared. The negative slat interference, discussed in the preceding paragraph, can be clearly seen for greater angles of attack, where the  $C_{l_{max}}$  value, for the three-element configuration, is lower than for the two element one. The maximum angle of attack calculated by the present numerical method was  $18^\circ$  for the two-element airfoil and  $20^\circ$  for the three-element configuration, showing the slat influence on the boundary-layer separation, over the main element upper surface.

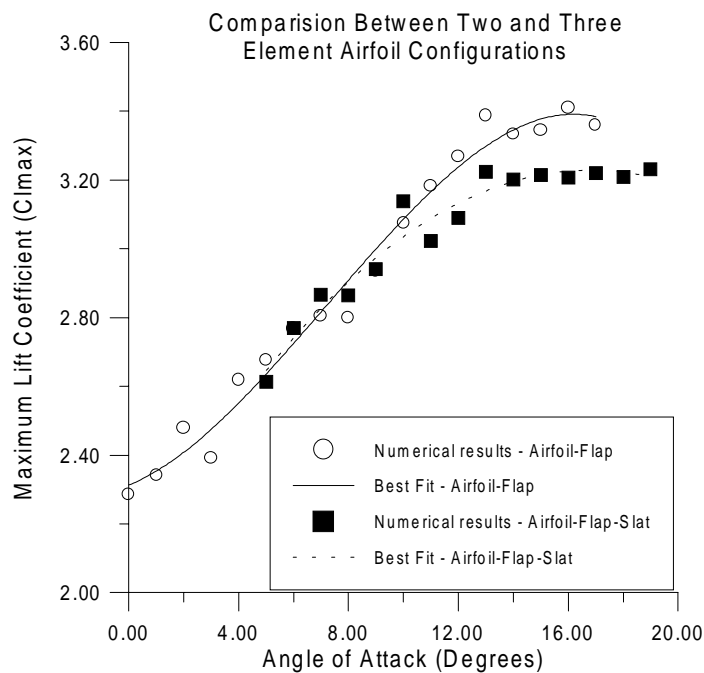


Figure – 8 Maximum lift coefficient for the two and the three element configurations

#### 4. FINAL REMARKS

The panel method used in this paper performs very well for a multi-element configuration, although some numerical problems were detected when the distance between two elements was very small. Such a kind of problem was solved by using constraints which do not allow these situations.

Some scattering can be observed in the numerical results and this is a consequence of the probabilistic character of the optimization technique employed in the present work. Another possible cause for the above problem is the set of constraints which has to be specified in order to obtain realistic solutions. Some times, conflicts among constraints can lead to bad solutions.

A consistent solution for the angle and the leading edge position of the flap was obtained for the two and three-element configurations. On the other hand, the results calculated for the slat seems to have some problem, because only small variations are observed for the angle and for the leading edge position. A possible explanation for this problem is the relatively low values considered for the configuration angle of attack. This limitation is a consequence of the constraint, which does not allow boundary-layer separation and, up to the highest angle of attack considered in this work, the slat was not necessary to delay separation on the main element upper surface. In this case, the slat interference decreases the configuration lift coefficient and, then, the optimization procedure searches for a position in which this interference is minimized.

#### 5. REFERENCES

- Bizarro, A.F., 1998, Interação Viscosa-não-Viscosa na Análise do escoamento em Grades Lineares de Máquinas de Fluxo. Tese de Mestrado, Instituto Tecnológico de Aeronáutica (ITA), S J Campos, SP, Brasil.
- Bristow, D.R. & Grose, G.G., 1978, Modification of the Douglas Neumann program to improve efficiency of predicting component interference and high lift characteristics. Washington, DC, NASA, (NASA CR-3020).
- Girardi, R.M., 1994, A Panel Method Based on Tangent Dipole Singularity for Internal and External Flows. *Boundary Elements Communications*, Vol. 5, No. 2, pp. 53-56.
- Girardi, R.M. & Bizarro, A.F., 1995, Modification of the Hess & Smith Method for calculating cascades and airfoils with cusped trailing edge, XIII Congresso Brasileiro de Engenharia Mecânica, 12 a 15 de Dezembro, Belo Horizonte, MG, Brasil.
- Girardi, R.M. & Silva Fo., D.E., 1994, Aerodynamic Study of a Three-Element Airfoil Configuration for An Automatic Flap Design. V Encontro Nacional de Ciências Térmicas (V-ENCIT), pp. 39-42, São Paulo, SP, Brasil.
- Hess, J.L. & Smith, A.M.O., 1966, Calculation of potential flow about arbitrary bodies. *Progress in Aeronautical Sciences*, Vol. 8, Pergamon Press.
- Hunt, B., 1978, The panel method for subsonic aerodynamic flows. VKI Lectures Series on *Compt. Fluid Dyn.*
- Lamb, H., 1932, *Hydrodynamics*. 6 ed., Cambridge, Cambridge University Press.
- Jacob, H. G., 1982, *Rechenergestuetzte Optimierung statischer und dynamischer Systeme*, Berin, Springer-Verlag.
- Rotta, J.C., 1971, Fortran IV, Rechenprogramm für Grenzschichten bei kompressiblen Ebenen und Achsensymmetrischen Strömungen, DLR FB 71-51, Göttingen, Germany.
- Schetz, J.A., 1984, *Foundations of Boundary Layer Theory for Momentum, heat and Mass Transfer*, Prentice-Hall Inc., Englewood Cliffs, New jersey, USA.